

Synthesis and characterization of spherical FeNi₃ metallic nanoparticles based on sodium dodecyl sulfate

Ozlem Altintas Yildirim^{a,b}, Mehmet Sahin Atas^{a*}

^aDepartment of Metallurgical and Materials Engineering, Konya Technical University, Konya, 42075, Turkey

^bNanotechnology and Advanced Materials Development, Application and Research Center, Konya Technical University, Konya, 42075, Turkey

(ORCID: 0000-0001-7867-7992), oayildirim@ktun.edu.tr

(ORCID: 0000-0001-8361-5913), msatas@ktun.edu.tr

Abstract

In this work, the metallic FeNi₃ nanoparticles with spherical structure have been synthesized in the presence of sodium dodecyl sulfate (SDS) using the hydrothermal method at 180 °C for 2 hours. The structural and morphological of the FeNi₃ metallic nanoparticles were characterized by X-ray diffraction (XRD), Fourier transforms infrared spectra (FTIR), scanning electron microscopy (SEM), and energy dispersion spectrum (EDS). As a result of XRD, the obtained metallic nanoparticles were observed to be single-phase pure stoichiometric FeNi₃ metallic nanoparticles with a face-centered cubic crystal structure. In the FTIR analysis, the peak obtained at 478.3 cm⁻¹ was a characteristic Fe-Ni peak. The SEM-EDS images obtained in the microstructure analysis showed that the FeNi₃ metallic nanoparticles produced were 169.33 nm in size and had a spherical morphology. The hydrothermal method used in the study is known to be very effective in producing metallic nanoparticles. In addition, the use of sodium dodecyl sulfate as an anionic surfactant and the realization of the reaction in ethanol/water environments reveal the innovative aspect of the study.

Keywords: Metallic nanoparticles, FeNi₃, hydrothermal method, sodium dodecyl sulfate.

1. Introduction

Recently, metallic nanoparticles (m-NPs) have been increasingly applied such as target drugs, magnetic fluid, electromagnetic devices, data storage, catalysis, temperature or humidity sensors, and so on [1-3]. It is known that the fascinating properties of low-dimensional (m-NPs) with different morphologies increase with the decrease in particle size [4, 5]. Therefore, precise design and control of morphological properties are required to stabilize m-NPs used in special applications [6-10]. Especially, Fe_xNi_{1-x} alloy, where x is in the range of 20-50% by weight, are m-NPs used in data storage [11], catalysis [12], temperature or humidity sensors [13, 14] or spintronic devices [8, 15, 16] and play a significant role in the progress of materials for green environmental. In this context, developing a low-cost synthesis procedure using simple laboratory equipment is synthesizing FeNi₃ m-NPs.

Until now, FeNi₃ m-NPs with various morphologies and size distributions have been produced with several approaches including mechanical alloying [17-19], anhydrous organometallic [20], spray pyrolysis [21], air melting [22], electrodeposition [23] and hydrothermal reduction [24-26]. One of these techniques, the hydrothermal method widely used in synthesizing various nanoparticles has been broadly built due to the superiority of simple operation, low cost, the simplicity of the equipment, and low synthesis temperature used during synthesis compared to other methods [27-31].

* Corresponding author.

E-mail addresses: msatas@ktun.edu.tr

DOI: 10.5281/zenodo.7472367

Received: 1 December 2022, Revised: 12 December 2022 and Accepted: 13 December 2022

ISSN: 2822-6054 All rights reserved.

However, the hydrothermal method to obtain FeNi₃ nanoparticles is not without problems, since it is difficult to convert iron salts to stable hydroxides during the hydrothermal reaction. Accordingly, the synthesis of FeNi₃ m-NPs remains a cautionary and not fully resolved issue. As a result, the basic parameters involved in these and similar chemical reactions need to be better optimized [24, 31, 32]. In the literature, FeNi₃ nanoparticles with different morphologies (sphere, sheet, rod, etc.) were produced by using a reducing agent as a hydrazine hydrate [33-35]. In Snoek's relationship, the magnetism can be increased importantly by producing nanoparticles with different morphologies [36]. FeNi₃ nano chains fabricated using cetyltrimethylammonium bromide (CTAB), as the cationic surfactant, showed a higher saturation magnetization (M_s) compared to particles with spherical morphology [37]. In addition, the addition of pyridinium and its derivatives to the reduction reaction resulted in the formation of 3-dimensional spine-like FeNi₃ structures as opposed to spherical particles [35]. Guo et al. investigated the influence of Sodium lignosulfonate (SLS) on the microstructure and crystallinity of FeNi₃ nanoparticles. It was observed that the transformation in FeNi₃ particle morphology was from spherical to flake-shaped by adding SLS to hydrazine reduction [38]. It is known that sodium dodecyl sulfate (SDS), which is an anionic surfactant, is used to synthesize FeNi₃ alloys through the hydrothermal method [27]. In studies so far, the influence of SDS use on the morphology, particle size, and shape of FeNi₃ m-NPs remains unclear.

There are few studies on hydrothermal synthesis using anionic surfactants (SDS) to calibrate the crystal structure, particle size, and shape of FeNi₃ m-NPs [29, 38, 39]. In addition, a detailed structural and morphological examination of the products synthesized in an ethanol/water environment using SDS was not done. In this work, the produce of FeNi₃ m-NPs using the hydrothermal synthesis method was synthesized using SDS, an anionic surfactant, into the hydrazine reduction solution in an ethanol/water medium, unlike the related studies.

2. Author Artwork (Material and Method)

2.1 Materials

Produce of FeNi₃ m-NPs by the hydrothermal method was actualized in a 150 mL Teflon-coated stainless-steel autoclave. FeNi₃ nanoparticles were synthesized by using Nickel (II) chloride hexahydrate (NiCl₂·6H₂O) (99.9%, Aldrich), Iron (III) nitrate nonahydrate (Fe(NO₃)₃·9H₂O) (98%, Aldrich), hydrazine hydrate (N₂H₄·H₂O, 80%, Aldrich), sodium dodecyl sulfate (SDS) (97.0%, Aldrich) and NaOH (96%, Aldrich). Ethanol (CH₃CH₂OH 96%, Aldrich) and pure water were used as a solvent.

2.2 Synthesis of FeNi₃ m-NPs

In the synthesis of m-NPs, the basic solution was prepared by first dissolving 0.41 g Fe(NO₃)₃·9H₂O and 0.71 g NiCl₂·6H₂O in 25 mL in ethanol-water (the volume ratio of ethanol/water 1:1) solution in amounts corresponding to 3:1 molar ratio of nickel to iron. After mechanically mixing the solution for 30 min., 0.1M NaOH was added dropwise to the constantly stirred solution at 0.20 mL/min speed until the pH reached to 11. Subsequently, 2 mL of hydrazine hydrate was dropped into the reaction as a reductant, and 0.5 g of SDS was used as a surfactant. For the prepared solution to be homogeneous, it was mixed vigorously in a magnetic stirrer at 25 °C for 30 minutes. The resulting solution (50 mL total volume) was placed in a 150 mL capacity Teflon-lined stainless-steel autoclave. The temperature of the hydrothermal device was raised to 180°C and kept there for 120 minutes. Subsequently, it was then left to cool to bring the temperature of the device to room temperature. The black m-NPs accumulated under the Teflon crucible were centrifuged at 10000 rpm for 5 minutes and separated in the solution. Afterward, the particles were washed several times with a 1:1 mixture of pure water and alcohol to remove alkali salts and/or impurities. Powders were obtained by drying in air at 40 °C for 4 hours without any additional heat treatment.

2.3 Characterization

The phase components and crystal structures of the resulting final powders were investigated using a Bruker D8 Advance model X-ray diffraction meter (XRD) with Cu-K α radiation ($\lambda = 1.54060 \text{ \AA}$) between $2\theta = 20\text{-}90^\circ$ limit values at a scanning rate of $2^\circ/\text{min}$ and an x-ray source operating voltage of 40 kV. Bond formations were investigated using Bruker VERTEX-70 model Fourier transform infrared spectra (FTIR) device. FTIR spectrum of the FeNi₃ m-NPs was recorded over the range of $4000\text{-}400 \text{ cm}^{-1}$ at a resolution of 4 cm^{-1} using FTIR spectroscopy. Elemental structures and morphologies of the obtained powders were characterized by using an SM Zeiss LS-10 model scanning electron microscope (SEM) equipped with energy-dispersive X-ray spectrometry (EDS).

3. Results and Discussion

3.1 Structural analysis

Phase analysis of FeNi₃ m-NPs produced in ethanol/water medium using surfactant SDS was performed by X-ray diffraction and is given in Fig. 1. The three diffraction peaks occurring at 2θ angle 44.1° , 51.5° and 75.8° correspond to the planes (111), (200) and (220) of cubic FeNi₃ according to JCPDS card of 65-3244 [4, 32]. The lattice parameter constant calculated from the peak at $2\theta = 44.1^\circ$ in the XRD diffraction pattern was determined as $a = 3.5547 \text{ \AA}$. This value is very close to 3.555 \AA of the FeNi₃ lattice parameter constant given in the JCPDS card. Moreover, in the XRD pattern, any diffraction peaks related to Fe and Ni oxides or other impurities were determined. The peaks of XRD diffraction pattern show that in the presence of SDS as an anionic surfactant, highly crystal FeNi₃ m-NPs can be successfully synthesized with the proposed hydrothermal technique [27, 38]. Liao et al., in their study on the manufacture of FeNi₃ alloy by hydrothermal method, examined the influence of the starting materials' Fe:Ni molar ratio on the products to be obtained. They showed that FeNi₃ nanoparticles can only be obtained in reactions with a 1:3 Fe:Ni molar ratio [27]. Therefore, our study chose the initial Fe:Ni molar ratio as 1:3, and FeNi₃ m-NPs were successfully obtained.

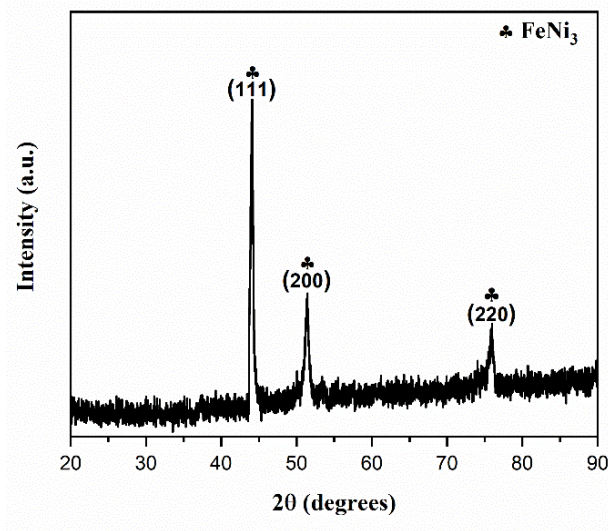


Fig. 1. XRD pattern of FeNi₃ nanoparticles.

The FTIR spectrum of the FeNi₃ m-NPs prepared with SDS in the ethanol/water medium in Fig. 2. The FT-IR spectrum showed one distinct peak look of 478.3 cm^{-1} which can be associated with the metallic bonds of Fe-Ni, Ni-Fe-Ni, or Fe-Ni-Ni groups [40, 41]. As a result, the FTIR (analysis) overlaps with the XRD diffraction pattern and confirms the hydrothermal method's successful production of FeNi₃ m-NPs.

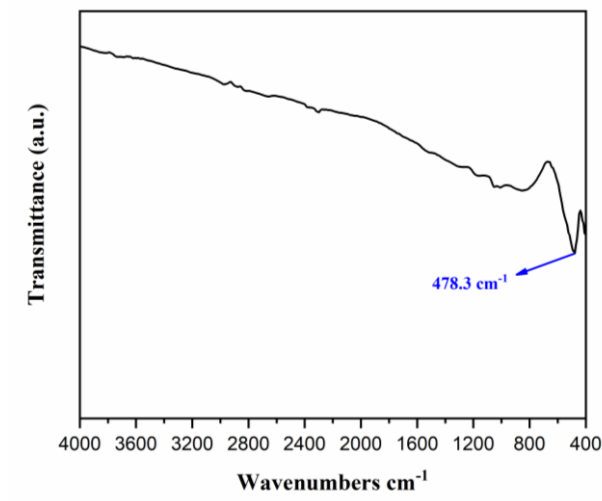


Fig. 2. FTIR spectra of FeNi₃ nanoparticles.

3.2 Morphological analysis

Fig. 3(a) and (b) show the SEM image and EDS analysis of FeNi₃ m-NPs obtained by the hydrothermal method, respectively. The SEM image given in Fig. 3(a) displays that FeNi₃ m-NPs had spherical morphology. The diameters of the spherical nanoparticles were examined with the Image-J program, and it was seen that the synthesized nanoparticles had an average radius of 169.33 nm. According to the literature review, it is seen that the morphology obtained is like the morphologies of FeNi₃ nanoparticles produced by the hydrothermal method [4, 32, 38].

The approximate elemental composition of the FeNi₃ m-NPs was determined by EDS in Fig. 3(b). Elemental analysis to determine the compositions revealed several well-defined energy lines of Fe and Ni. The atomic contents of Iron and Nickel were found to be 27.30% and 72.70%, respectively, and an atomic ratio of 2.67 was obtained, which is close to the ratio of Fe:Ni in FeNi₃ alloys. The differences in the precursor composition probably originate from the exhaust in the hydrothermal solution. This atomic ratio indicates that the synthesis of FeNi₃ nanoparticles has been accomplished.

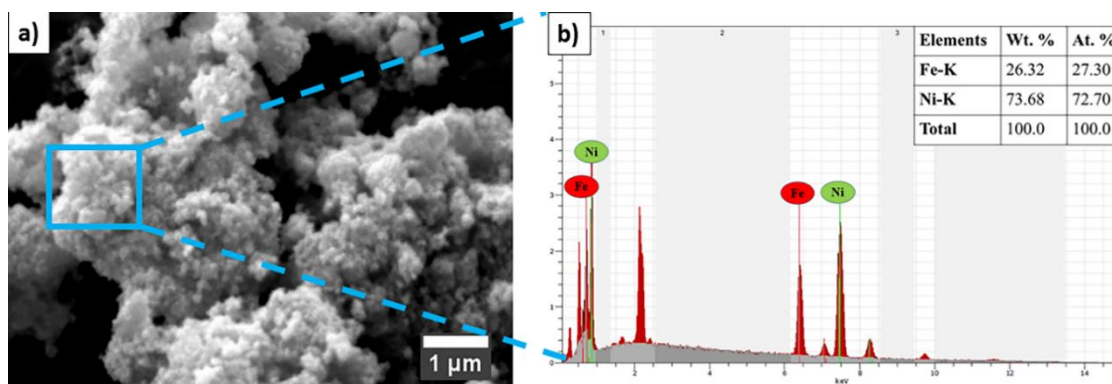


Fig. 3. (a) SEM image and (b) EDS spectra of FeNi₃ m-NPs.

The synthesis of FeNi₃ m-NPs was carried out via a simple hydrothermal technique using a 1:3 initial precursor composition of Fe and Ni salt mixture to provide a synthesis of only FeNi₃ m-NPs without the formation of any oxide or metallic forms of these metals. To determine the chemical structure and elemental

distribution of m-NPs produced by the hydrothermal method in more detail, an elemental mapping analysis of the region in the SEM image was performed. Elemental mapping analysis of the produced nanoparticles is given in Fig. 4. Fig. 4(a) shows the SEM micrograph of the region where elemental mapping was performed. In the elemental mapping analysis, it is seen in Fig. 4(b) that Ni and Fe elements are homogeneously distributed in the spherical m-NPs. According to the elemental mapping images in Fig. 4(c-d), it can be understood from the color intensities of the elements that while the Ni element is found in a dense proportion in the spherical particles, the Fe element is in a lower proportion compared to Ni.

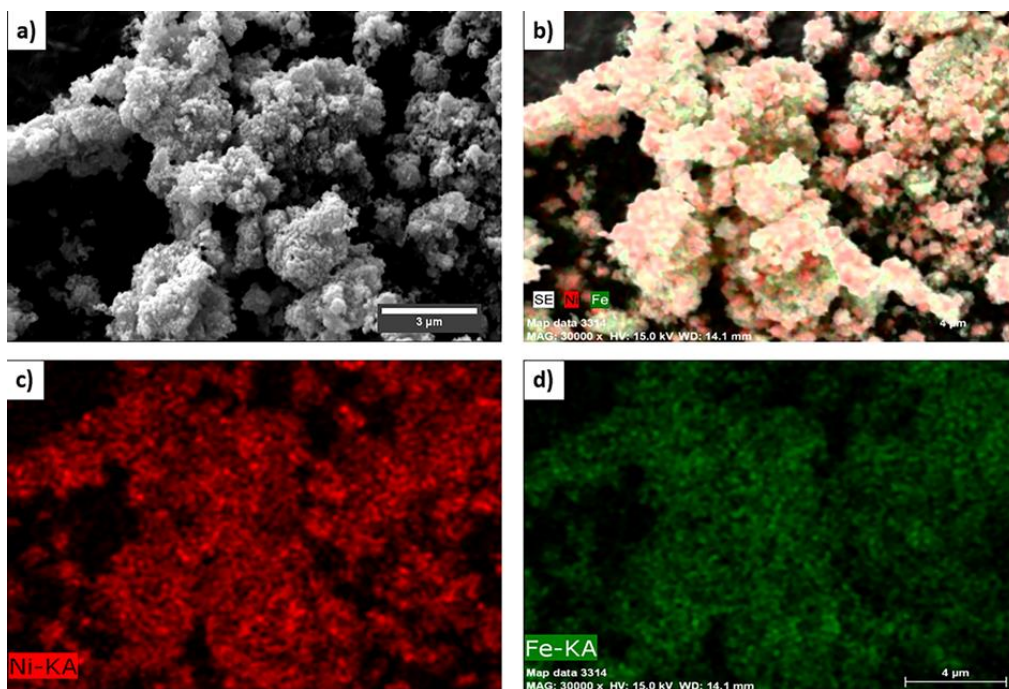
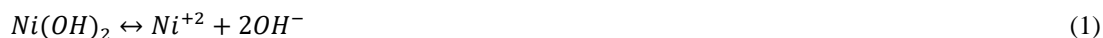


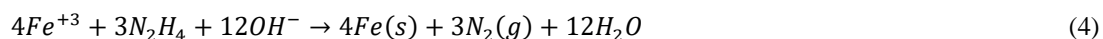
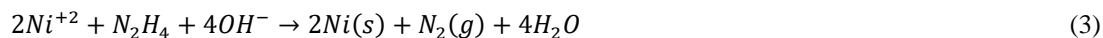
Fig. 4. (a) SEM image, (b-d) elemental mapping images of FeNi₃ m-NPs.

3.3 Formation mechanisms of the FeNi₃ m-NPs

Based on the results obtained, the synthesis mechanism of FeNi₃ m-NPs is explained as follows [24, 25, 27]. In the first step, when NaOH is slowly added to the solution prepared from Fe (Fe(NO₃)₃·9H₂O) and Ni (NiCl₂·6H₂O) salts, the hydroxide form M(OH)₂ (M=Ni, Fe) is formed. If the (Fe⁺³/Fe) and (Ni⁺²/Ni) ratios are close in the solution medium, solid Fe(OH)₂ and Ni(OH)₂ are decomposed to form Fe⁺³ and Ni⁺² ionic forms with the reactions shown in Equations 1 and 2 as follow:



Then, with the effect of hydrazine hydrate (N₂H₄·H₂O) and SDS added to the solution, Fe⁺³ and Ni⁺² ions form metallic Fe and Ni atoms as shown in Equations 3 and 4.



Finally, metallic atoms in the solution medium interact to form Fe-Ni alloy nuclei as shown in Equation 5.



In Equation (1-5), it is known that Fe and Ni salts in the intensely basic medium are reduced by hydrazine hydrate during the formation of FeNi₃ nanoparticles. Hydrazine hydrate (N₂H₄.H₂O) is known to be a Lewis base. Hydrazine hydrate decomposes in aqueous medium as in the equation below [42, 43]:



Results showed that in the absence of surfactant, FCC FeNi₃ nuclei were randomly formed by homogeneous nucleation [44]. Studies in the literature have shown that surfactants have superior abilities to form particles in a morphological and size-controlled style [45]. The cores of m-NPs are formed from the interaction between Fe/Ni ions and the sulphonic groups of the surfactant (SDS). SDS serves as a template for the growth of FeNi₃ m-NPs with spherical morphology [46].

4. Conclusion

The spherical FeNi₃ m-NP was successfully produced using the hydrothermal method via hydrazine reduction at the ambient condition in the presence of SDS, and the following conclusions can be drawn:

- According to XRD analysis, FeNi₃ m-NPs have been synthesized without the formation of any oxide or metallic forms of Fe and Ni metals.
- FTIR analysis revealed a vibration peak showing the presence of Fe-Ni, Ni-Fe-Ni, or Fe-Ni-Ni group metallic bonds, which indicates the formation of the m-NPs.
- SEM and EDS analyses show that spherical FeNi₃ m-NPs have approximately 169.33 nm average grain size.
- Elemental mapping images of Fe and Ni elements provide that homogeneous distribution of these elements through FeNi₃ m-NPs.

Such a hydrothermal synthesis route of m-NPs can open the door for designing a new class of other m-NPs with different sizes and morphologies for various potential application fields.

Author Contribution Statement

Mehmet Sahin Atas: Conceptualization, Methodology, Writing – original draft, Investigation, Writing – review & editing. **Ozlem Altintas Yildirim:** Investigation, Methodology, Writing – review & editing.

Acknowledgments

The authors gratefully acknowledge Ozkan Uzum and Mustafa Celik for their assistance with SEM analyses.

References

- [1] M. Ashtiani, S.H. Hashemabadi, A. Ghaffari, A review on the magnetorheological fluid preparation and stabilization, *Journal of Magnetism and Magnetic Materials*, 374 (2015) 716-730.
- [2] M. Jalali, S. Dauterstedt, A. Michaud, R. Wuthrich, Electromagnetic shielding of polymer–matrix composites with metallic nanoparticles, *Composites Part B: Engineering*, 42 (2011) 1420-1426.
- [3] Y. Liu, S. Litière, E.G.E. de Vries, D. Sargent, L. Shankar, J. Bogaerts, L. Seymour, The role of response evaluation criteria in solid tumour in anticancer treatment evaluation: Results of a survey in the oncology community, *European Journal of Cancer*, 50 (2014) 260-266.

- [4] Y.-C. Chen, F.-C. Zheng, Y.-L. Min, T. Wang, Y.-G. Zhao, Synthesis and properties of magnetic FeNi₃ alloyed microchains obtained by hydrothermal reduction, *Solid state sciences*, 14 (2012) 809-813.
- [5] E.V. Shevchenko, D.V. Talapin, N.A. Kotov, S. O'Brien, C.B. Murray, Structural diversity in binary nanoparticle superlattices, *Nature*, 439 (2006) 55-59.
- [6] M.P. Fernández-García, P. Gorria, M. Sevilla, M.P. Proenca, R. Boada, J. Chaboy, A.B. Fuertes, J.A. Blanco, Enhanced protection of carbon-encapsulated magnetic nickel nanoparticles through a sucrose-based synthetic strategy, *The Journal of Physical Chemistry C*, 115 (2011) 5294-5300.
- [7] Y.I. Golovin, D.Y. Golovin, A.V. Shuklinov, R.A. Stolyarov, V.M. Vasyukov, Electrodeposition of nickel nanoparticles onto multiwalled carbon nanotubes, *Technical Physics Letters*, 37 (2011) 253-255.
- [8] Y. Liu, Y. Chi, S. Shan, J. Yin, J. Luo, C.-J. Zhong, Characterization of magnetic NiFe nanoparticles with controlled bimetallic composition, *Journal of alloys and compounds*, 587 (2014) 260-266.
- [9] Y. Mao, J. Parsons, J.S. McCloy, Magnetic properties of double perovskite La₂BmO₆ (B= Ni or Co) nanoparticles, *Nanoscale*, 5 (2013) 4720-4728.
- [10] N. Rinaldi-Montes, P. Gorria, D. Martínez-Blanco, A. Fuertes, L.F. Barquín, J.R. Fernández, I. de Pedro, M. Fdez-Gubieda, J. Alonso, L. Olivi, Interplay between microstructure and magnetism in NiO nanoparticles: breakdown of the antiferromagnetic order, *Nanoscale*, 6 (2014) 457-465.
- [11] S. Moustafa, W. Daoush, Synthesis of nano-sized Fe-Ni powder by chemical process for magnetic applications, *Journal of materials processing technology*, 181 (2007) 59-63.
- [12] J.-M. Yan, X.-B. Zhang, S. Han, H. Shioyama, Q. Xu, Magnetically recyclable Fe-Ni alloy catalyzed dehydrogenation of ammonia borane in aqueous solution under ambient atmosphere, *Journal of Power Sources*, 194 (2009) 478-481.
- [13] A. Djekoun, N. Boudinar, A. Chebli, A. Otmani, M. Benabdeslem, B. Bouzabata, J. Greneche, Structure and magnetic properties of Fe-rich nanostructured Fe_{100-x}Ni_x powders obtained by mechanical alloying, *Physics Procedia*, 2 (2009) 693-700.
- [14] S. Vitta, A. Khuntia, G. Ravikumar, D. Bahadur, Electrical and magnetic properties of nanocrystalline Fe_{100-x}Ni_x alloys, *Journal of magnetism and magnetic materials*, 320 (2008) 182-189.
- [15] Y.I. Golovin, R. Stolyarov, A. Shuklinov, Morphology and growth kinetics of Ni nanoparticles on the surface of multiwalled carbon nanotubes at galvanostatic electrodeposition, *Technical Physics*, 58 (2013) 1189-1193.
- [16] J.T. Tian, C.H. Gong, L.G. Yu, Z.S. Wu, Z.J. Zhang, Synthesis of dandelion-like three-dimensional nickel nanostructures via solvothermal route, *Chinese Chemical Letters*, 19 (2008) 1123-1126.
- [17] B. Zeifert, J. Salmones, J. Hernández, R. Reynoso, N. Nava, J. Cabañas-Moreno, G. Aguilar-Ríos, Preparation of iron-nickel catalysts by mechanical alloying, *Materials Letters*, 43 (2000) 244-248.
- [18] I. Chicinas, O. Geoffroy, O. Isnard, V. Pop, Soft magnetic composite based on mechanically alloyed nanocrystalline Ni₃Fe phase, *Journal of Magnetism and Magnetic Materials*, 290 (2005) 1531-1534.
- [19] I. Chicinas, V. Pop, O. Isnard, J. Le Breton, J. Juraszek, Synthesis and magnetic properties of Ni₃Fe intermetallic compound obtained by mechanical alloying, *Journal of alloys and compounds*, 352 (2003) 34-40.
- [20] Y. Chen, X. Luo, G.-H. Yue, X. Luo, D.-L. Peng, Synthesis of iron-nickel nanoparticles via a nonaqueous organometallic route, *Materials Chemistry and Physics*, 113 (2009) 412-416.
- [21] S. Eroglu, S. Zhang, G. Messing, Synthesis of nanocrystalline Ni-Fe alloy powders by spray pyrolysis, *Journal of materials research*, 11 (1996) 2131-2134.
- [22] Y.-H. Zhou, M. Harmelin, J. Bigot, Sintering behaviour of ultra-fine Fe, Ni and Fe-25wt% Ni powders, *Scripta metallurgica*, 23 (1989) 1391-1396.
- [23] S.-H. Kim, H.-J. Sohn, Y.-C. Joo, Y.-W. Kim, T.-H. Yim, H.-Y. Lee, T. Kang, Effect of saccharin addition on the microstructure of electrodeposited Fe-36 wt.% Ni alloy, *Surface and Coatings Technology*, 199 (2005) 43-48.
- [24] L. Liu, J. Guan, W. Shi, Z. Sun, J. Zhao, Facile synthesis and growth mechanism of flowerlike Ni-Fe alloy nanostructures, *The Journal of Physical Chemistry C*, 114 (2010) 13565-13570.
- [25] M.L. Yuan, J.H. Tao, L. Yu, C. Song, G.Z. Qiu, Y. Li, Z.H. Xu, Synthesis and magnetic properties of Fe-Ni alloy nanoparticles obtained by hydrothermal reaction, in: *Advanced Materials Research*, Trans Tech Publ, 2011, pp. 748-753.

- [26] M.Ş. Ataş, Ö.A. Yildirim, Ni-FeNi₃-Fe₃O₄ Synthesis and Characterization of Ni-FeNi₃-Fe₃O₄ Metallic Nanoalloys by Hydrothermal Method, *Konya Journal of Engineering Sciences*, 10 965-975.
- [27] Q. Liao, R. Tannenbaum, Z.L. Wang, Synthesis of FeNi₃ alloyed nanoparticles by hydrothermal reduction, *The Journal of Physical Chemistry B*, 110 (2006) 14262-14265.
- [28] A. Bouremana, A. Guittoum, M. Hemmous, B. Rahal, J.J. Sunol, D. Martínez-Blanco, J.A. Blanco, P. Gorria, N. Benrekaa, J. Magn. Magn. Mater., 11 (2014) 358.
- [29] H. Chen, C. Xu, G. Zhao, Y. Liu, Template-free formation of urchin-like FeNi₃ microstructures by hydrothermal reduction, *Materials Letters*, 91 (2013) 75-77.
- [30] A. Bouremana, A. Guittoum, M. Hemmous, D. Martínez-Blanco, P. Gorria, J.A. Blanco, N. Benrekaa, Microstructure, morphology and magnetic properties of Ni nanoparticles synthesized by hydrothermal method, *Materials Chemistry and Physics*, 160 (2015) 435-439.
- [31] X. Su, H. Zheng, Z. Yang, Y. Zhu, A. Pan, Preparation of nanosized particles of FeNi and FeCo alloy in solution, *Journal of materials science*, 38 (2003) 4581-4585.
- [32] A. Bouremana, A. Guittoum, M. Hemmous, D. Martínez-Blanco, P. Gorria, J. Blanco, Low temperature hydrothermal synthesis of Ni₇₅Fe₂₅ nanostructured powders: Microstructure, morphology and magnetic behaviour, *Journal of Magnetism and Magnetic Materials*, 466 (2018) 212-218.
- [33] X. Lu, G. Liang, Y. Zhang, Synthesis and characterization of magnetic FeNi₃ particles obtained by hydrazine reduction in aqueous solution, *Materials Science and Engineering: B*, 139 (2007) 124-127.
- [34] H. Wang, J. Li, X. Kou, L. Zhang, Synthesis and characterizations of size-controlled FeNi₃ nanoplatelets, *Journal of Crystal Growth*, 310 (2008) 3072-3076.
- [35] X. Lu, G. Huo, X. Liu, G. Liang, Z. Han, X. Song, Hierarchical FeNi₃ assemblies with caltrop-like architectures: synthesis, formation mechanism and magnetic properties, *CrystEngComm*, 14 (2012) 5622-5626.
- [36] R. Walser, W. Win, P. Valanju, Shape-optimized ferromagnetic particles with maximum theoretical microwave susceptibility, *IEEE transactions on magnetics*, 34 (1998) 1390-1392.
- [37] X. Lu, Q. Liu, G. Huo, G. Liang, Q. Sun, X. Song, CTAB-mediated synthesis of iron-nickel alloy nano chains and their magnetic properties, *Colloids and Surfaces A: Physicochemical and Engineering Aspects*, 407 (2012) 23-28.
- [38] H. Guo, M. Li, Z. Qin, F. Li, X. Zhang, W. Wu, H. Cheng, Shape-controlled synthesis of flake-like FeNi₃ nanoparticles based on sodium lignosulfonate, *Advanced Powder Technology*, 32 (2021) 755-763.
- [39] G. Hongxia, C. Hua, L. Fan, Q. Zhenping, C. Suping, N. Zuoren, Shape-controlled synthesis of FeNi₃ nanoparticles by ambient chemical reduction and their magnetic properties, *Journal of Materials Research*, 27 (2012) 1522-1530.
- [40] M. Khodadadi, A.H. Panahi, T.J. Al-Musawi, M. Ehrampoush, A. Mahvi, The catalytic activity of FeNi₃@SiO₂ magnetic nanoparticles for the degradation of tetracycline in the heterogeneous Fenton-like treatment method, *Journal of Water Process Engineering*, 32 (2019) 100943.
- [41] N. Nasseh, F.S. Arghavan, S. Rodriguez-Couto, A. Hossein Panahi, Synthesis of FeNi₃/SiO₂/CuS magnetic nano-composite as a novel adsorbent for Congo Red dye removal, *International Journal of Environmental Analytical Chemistry*, (2020) 1-21.
- [42] K. Yu, D.J. Kim, H.S. Chung, H. Liang, Dispersed rodlike nickel powder synthesized by modified polyol process, *Materials Letters*, 57 (2003) 3992-3997.
- [43] N. Xiaomin, S. Xiaobo, Z. Huagui, Z. Dongen, Y. Dandan, Z. Qingbiao, Studies on the one-step preparation of iron nanoparticles in solution, *Journal of Crystal Growth*, 275 (2005) 548-553.
- [44] M. Norgren, H. Edlund, Lignin: Recent advances and emerging applications, *Current Opinion in Colloid & Interface Science*, 19 (2014) 409-416.
- [45] A. Barhoum, H. Rahier, R.E. Abou-Zaied, M. Rehan, T. Dufour, G. Hill, A. Dufresne, Effect of Cationic and Anionic Surfactants on the Application of Calcium Carbonate Nanoparticles in Paper Coating, *ACS Applied Materials & Interfaces*, 6 (2014) 2734-2744.
- [46] P. Taylor, Ostwald ripening in emulsions, *Advances in Colloid and Interface Science*, 75 (1998) 107-163.